Bone Reports 17 (2022) 101611

Contents lists available at ScienceDirect

Bone Reports

journal homepage: www.elsevier.com/locate/bonr

Cranial reconstruction evaluation - comparison of European statistical shape model performance on Chinese dataset

Marc Anton Fuessinger [a,*], Marc Christian Metzger [a], Rene Rothweiler [a], Leonard Simon Brandenburg [a], Stefan Schlager [b]

[a] Department of Oral and Maxillofacial Surgery, Albert-Ludwigs University Freiburg, Hugstetterstr. 55, 79106 Freiburg, Germany
[b] Department of Physical Anthropology, Albert-Ludwigs University Freiburg, Hebelstr. 29, 79104 Freiburg, Germany

ARTICLE INFO

Keywords:
Statistical shape model (SSM)
Computer-assisted surgery (CAS)
Virtual defect reconstruction
3D planning
Virtual planning
Skull defects
Ethnicity

ABSTRACT

Purpose: Morphological variability of the skull is an important consideration for cranioplasty and implant design. Differences in morphology of the skull based on the ethnicity are known. In a previous study we could show the accuracy and benefits of virtual reconstructions based on a statistical shape model (SSM) for neurocranial defects. As the SSM is trained on European data, the question arises how well this model fares when dealing with patients with a different ethnic background. In this study we aim to evaluate the accuracy and applicability of our proposed method when deploying a cranial SSM generated from European data to estimate missing parts of the neurocranium in a Chinese population.

Methods: We used the same data and methods as in our previous study and compared the outcomes when applied to Chinese individuals. A large unilateral defect on the right side and a bilateral defect were created. The outer surface of the cranial table was reconstructed from CT scans, meshed with triangular elements, and registered to a template. Principal component analysis together with Thin Plate Spines (TPS) deformation was applied to quantify modes of variation. The mesh to mesh distances between the original defects´ surfaces and the reconstructed surface were computed.

Results: Comparing the Chinese test group with the European control group, regarding the entire defect the analysis shows no significant difference for unilateral defects (test vs. control group/0.46 mm ± vs. 0.44 mm). Reconstruction of bilateral defects exhibited only in slightly higher prediction errors than those of unilateral defects (0.49 mm ± vs. 0.45 mm).

Conclusion: The proposed method shows a high accuracy that seems to be ethnical independent - with low error margins for virtual skull reconstruction and implant design.

Clinical relevance: Metallic objects may severely impact image quality in several CBCT devices.

1. Introduction

Neurosurgical procedures often involve reconstruction of skull defects caused by trauma, tumors, congenital deformities, or postoperative defects (Mitchell et al., 2020; Piazza and Grady, 2017). Reasons to repair the defects are protection of intracerebral structures, ensuring the cerebrospinal fluid (CSF) flow dynamics and restoring of the facial appearance to avoid a sunken flap (Piazza and Grady, 2017). This asymmetric appearance can have strong implications on the psychological constitution of the patient. The patient and the surrounding will benefit from a precise restoration of the previous appearance and re-establishing the protective barrier. For large defects, computer-designed implants from computed tomographic reconstructions are expensive but effective for complex skull defects (Chim and Schantz, 2005). These precise prostheses show a high accuracy, ease and fit without the requirement of indirect modeling based on life-size models. Eufinger and Wehmoller achieved a precision of 0.25 mm with the prefabrication of titanium implants using a direct method (Eufinger and Wehmoller, 1998).

Cranioplasty has a long surgical history, but new techniques and new material options have led to the question how to improve the virtual reconstruction of the skull to design implants for cranioplasty (Mashiko

* Corresponding author at: Albert-Ludwigs University Freiburg, Hugstetterstr. 55, 79106 Freiburg, Germany.
E-mail addresses: marc.anton.fuessinger@uniklinik-freiburg.de (M.A. Fuessinger), marc.metzger@uniklinik-freiburg.de (M.C. Metzger), rene.rothweiler@uniklinik-freiburg.de (R. Rothweiler), leonard.brandenburg@uniklinik-freiburg.de (L.S. Brandenburg), stefan.schlager@anthropologie.uni-freiburg.de (S. Schlager).

https://doi.org/10.1016/j.bonr.2022.101611
Received 5 March 2022; Received in revised form 10 August 2022; Accepted 12 August 2022
Available online 13 August 2022

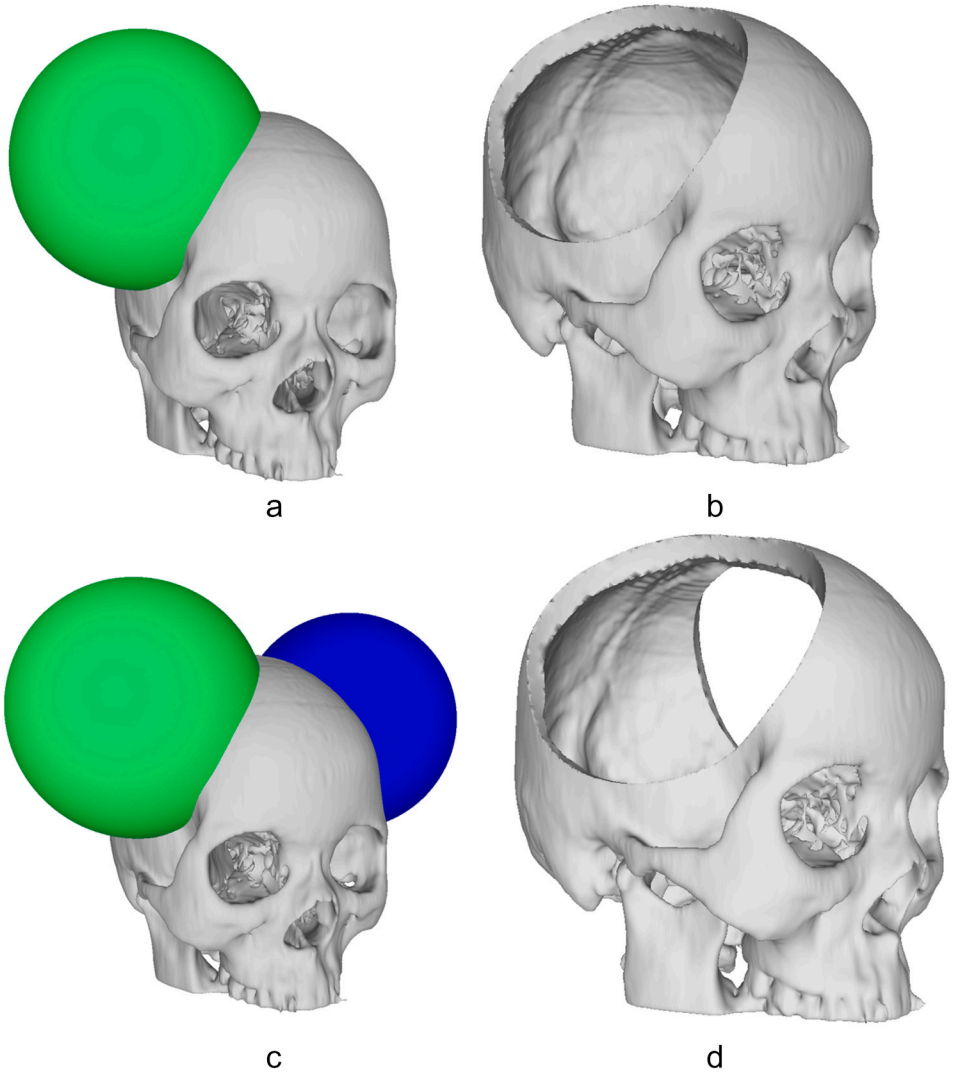

Fig. 1. a, b, c, d: Creation of uni- and bilateral defect: Spheres of 5 cm radius, with their center located at the temporal bone.

et al., 2019). Especially the time-demanding computer-aided design (CAD) step is challenging and reduces the cost-effectiveness of this technique. As shown, statistical shape models (SSM) can facilitate the construction steps by automatization in different anatomical regions (Bredbenner et al., 2010; Fuessinger et al., 2018, 2019; Galloway et al., 2013; Mutsvangwa et al., 2015; Zhang et al., 2018). SSM also enables the reconstruction of bilateral defects that could not be reconstructed automatically by the mirroring technique, which is the gold standard to date (Fuessinger et al., 2019). In this study we employ a SSM that was created from a European training sample in order to capture the three-dimensional shape variability of the cranial vault in healthy European adults.

The question arises whether the model trained on adult Europeans can be applied to other ethnicities and, above all, how this affects the resulting reconstruction accuracy.

It is a well-known fact that ethnicity explains variability in cranial morphology (Agbolade et al., 2020; Bravo-Hammett et al., 2020; Dao Trong et al., 2020). Cranial shape variability is in fact used for evaluating ethnic association in a forensic or archaeological context. Variabilities are described between native American groups, Asians, and Caucasians. The claimed variability influences the surgical planning and treatment (Dao Trong et al., 2020; de Azevedo et al., 2017; Elliott and Collard, 2009; Galland and Friess, 2016; Harvati and Weaver, 2006; Hubbe et al., 2015).

Given that morphological differentiation and diversity between modern human populations, the present study aims to investigate whether our approach, relying on a SSM generated from European individuals, is suitable for estimating neurocranial defects in a different ethnic population, such as a South-Eastern Chinese sample. To approach this question, we will compare the results of the reconstruction of virtual skull defects in a Chinese population to the known results of the reconstruction of European skulls (Fuessinger et al., 2018).

2. Material and methods

As this is an evaluation of a previously published method on a new dataset, the relevant procedures will only be outlined briefly and the interested reader is encouraged to find more details in the original article (Fuessinger et al., 2018).

Our approach consists of a data-driven reconstruction of cranial defects based on a SSM, with a Thin-Plate deformation utilizing geometric morphometric methods (GMM) to improve the final. The used SSM incorporates empirical knowledge about the shape variability of a healthy sample for reconstructing the cranial shape.

All statistical analysis, as well as image registration and shape modeling were performed using the open-source statistical/mathematical platform R – and more specifically the R-packages ANTsR, Morpho, Rvcg, mesheR and RvtkStatismo (Goodall, 1991; Lüthi et al., 2009,

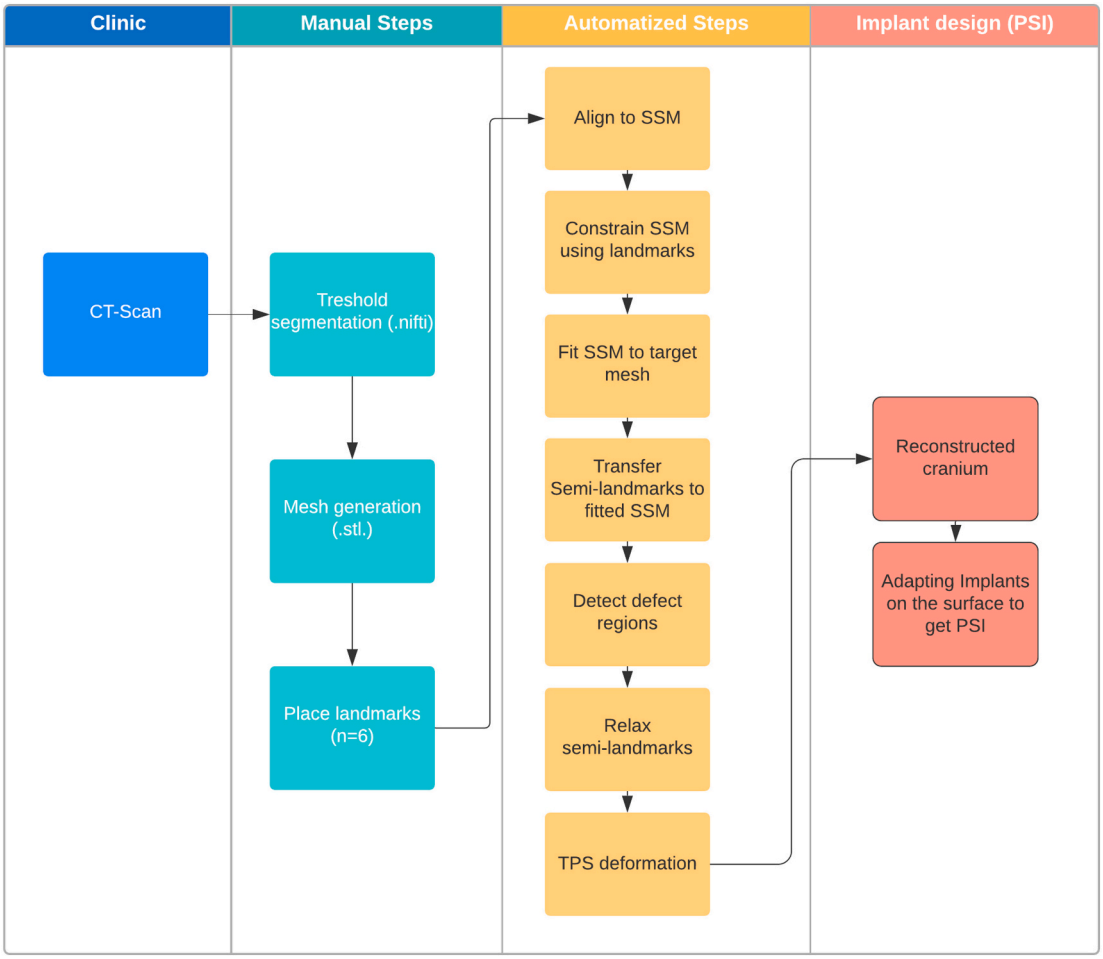

Fig. 2. Proposed workflow for reconstruction of cranial defects.

2012; R Development Core Team, 2011; Schlager and Rüdell, 2015).

2.1. Statistical shape model

We used the same SSM of the cranial vault of European adults as in (Fuessinger et al., 2018; Semper-Hogg et al., 2017, p.) that has been is generated from 131 craniofacial CT scans of pathologically unaffected patients ($n = 61$ female, $n = 70$ male patients, average age = 53.2 years). The average slice thickness of the CT scans was 1.2 mm. For generating the SSM, the DICOM data were segmented using a grey-value thresholding to extract the osseous structure. Segmentation was performed in 3D Slicer (Fedorov et al., 2012). After the segmentation a sparse set of well-defined anatomical landmarks was placed on all landmarks to obtain initial spatial correspondence. Based on these correspondences, the image data was aligned to a template skull and then elastically registered using the R-package ANTsR. A surface mesh of the template was then deformed according to the resulting deformation. To allow for more local variability and to obtain are more accurate correspondence, the deformed mesh was then mapped to a surface representation of the target. As a result, we obtained 131 skull meshes with corresponding vertices. These were then rigidly aligned to a common coordinate system and a PCA model was computed using the software package RvtkStatismo. For further details on SSM generation, see (Fuessinger et al., 2018).

2.2. Testing sample

The testing sets comprise CT-scans of 33 pathologically unaffected Chinese crania (age: 28 + 14 years, female 26 females; 7 males; 33 subjects) and 33 healthy European crania (age: 35 + 12 years, 24 females, 9 males; 33 subjects) – with the latter being the same testing data used in (Fuessinger et al., 2018). The skulls were classified as pathologically unaffected if they did not present any morphological feature of diseases, such as fractures or neoplasia. All scans were taken during medical treatment.

2.3. Creation of artificial defects

In order to create virtual bony defects of the right and left temporal bone, the CT-scans of the testing data were threshold segmented and triangular mesh representation of the cranium generated. The latter were subsequently imported into the open software Blender (Bruns, 2020). For creating cranial defects on those meshes, a sphere with a radius of 5 cm was placed at the temporal bone and the part of the surface mesh representing the cranium lying within the sphere was removed by a Boolean operation (Fig. 1a & b).

Additionally, bilateral defects were created by performing the procedure on both sides (Fig. 1c & d).

2.4. Data processing

The workflow (Fig. 2) consists of two parts:

The first (manual) part consists in placing six landmarks (nasion, zygomatico-frontal suture (both sides), external acoustic meatus (both sides), and external occipital protuberance) throughout the

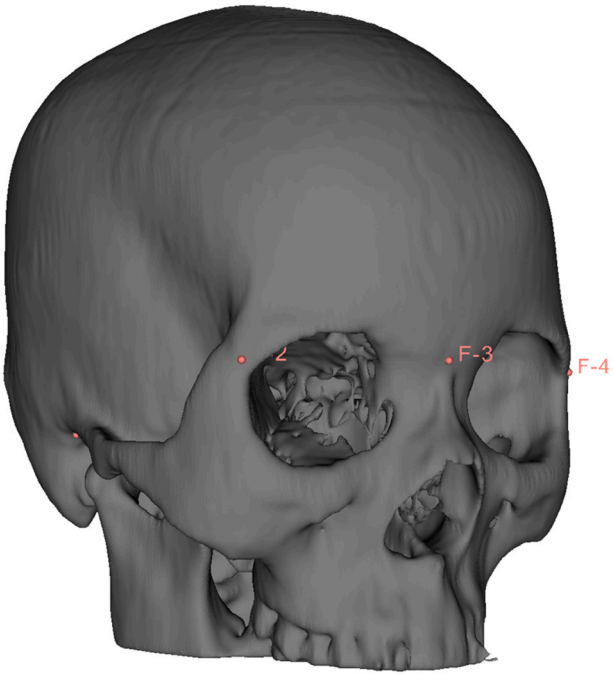

Fig. 3. Placing six landmarks on a patient skull for roughly registration of the SSM [nasion, zygomatico-frontal suture (both sides), external acoustic meatus (both sides), and external occipital protuberance].

testing sample using the "markup" module in 3D Slicer (Fig. 3) (Kikinis et al., 2014; Kim et al., 2012). The mentioned landmarks serve to establish an initial correspondence between the target shape and the SSM and to constrain the SSM accordingly.

The second part consists in the fully automatic reconstruction of the cranial vault by finding a suitable SSM instance and warping that to the defect target surface (see Fuessinger et al. (2018) for details).

2.5. Evaluation

Reconstruction accuracy is analyzed on the outer surface of the cranial table to estimate the general error, as well as the error specific to the defect's border, by computing the average per-vertex distances from the defective part to the reconstruction (Fig. 4). The border itself was determined by finding those vertices located on the outer table along the edges of the mesh surrounding the defect. For each of the reconstructions, we calculated the mean error, the maximum error, and the number of vertices within the reconstructed area with an error of less than 1 mm. The selected error metric was chosen to make the results comparable with previous articles on virtual reconstruction methods (Fuessinger et al., 2018; Marreiros et al., 2016). Given the fact that the minimum Slice-thickness in clinical data is often around 1 mm, an actual error below this value could be viewed as within the uncertainty inherent in the image data.

While the general error represents the overall fit of the reconstructed surface, the error at the defects' borders are important for implant design as a close fit as possible is needed for a smooth placement of the implant. The error was evaluated both on the unilateral and on the bilateral virtual defects. Statistical significance between samples was assessed using a student *t*-test for mean and maximum errors and a permutation test for the median regarding the percentage below 1 mm, as the latter is not normally distributed.

3. Results

Due to the clinical application of the SSM, the evaluation focuses on the reconstruction error on the outer surface and, especially for the implant design, on the defect interface.

Fig. 5a shows the error distribution for all cases.

3.1. Unilateral defect

Regarding the general error, there is no significant difference between populations. With both populations showing a very low average error rate with a mean error of 0.51 mm (SD = 0.17) in Chinese and 0.46 mm (SD = 0.16) in Europeans. The same is true for the maximum errors. For the entire defect, no difference between both groups can be shown (Fig. 5b). Additionally, the distribution of the error values of vertices that are below an error of 1 mm was analyzed. The median of this value is 0.89 in Chinese and 0.88 in Europeans.

Fig. 5c suggests that there is no statistically significant difference between the Asian and Caucasian population regarding the percentage of vertices below 1 mm throughout the entire defect. That impression could be proved by the permutation testing.

Analyzing the error distribution at the borders of the defect, the diagrams tell a slightly different story (Fig. 6). In both cases, uni- and bilateral defects, there is a significant difference between both

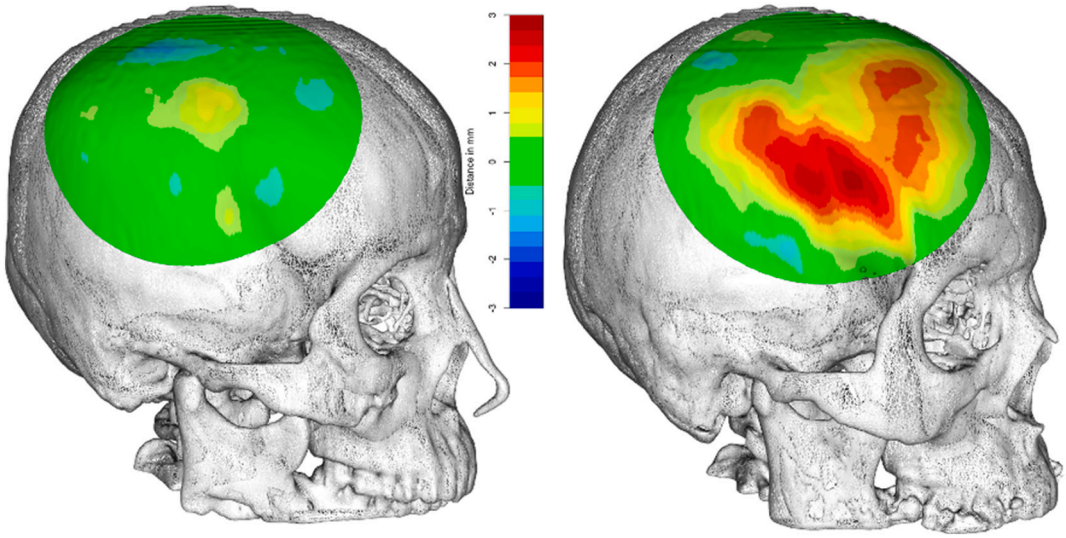

Fig. 4. Visual 3D evaluation (best (left) and worst (right) Chinese reconstruction result) showing the per-vertex deviation in mm

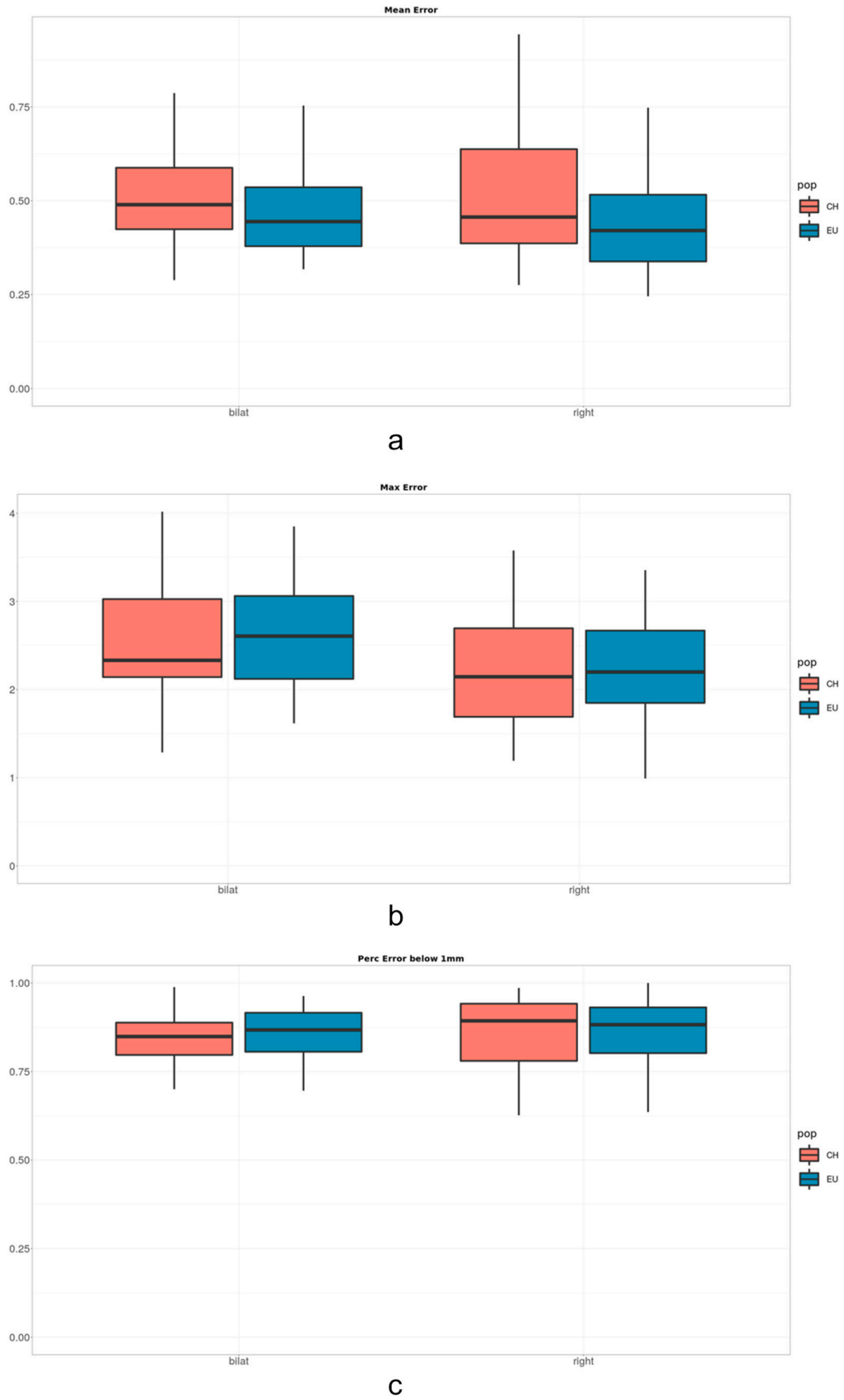

Fig. 5. Boxplots visualizing the reconstruction error distribution of the entire defect for both groups divided up in uni- and bilateral defects in mm.
Mean error distribution of the error distribution; (b) Maximum error distribution of the error distribution (c) Percentage of vertices below 1 mm of the entire defect.

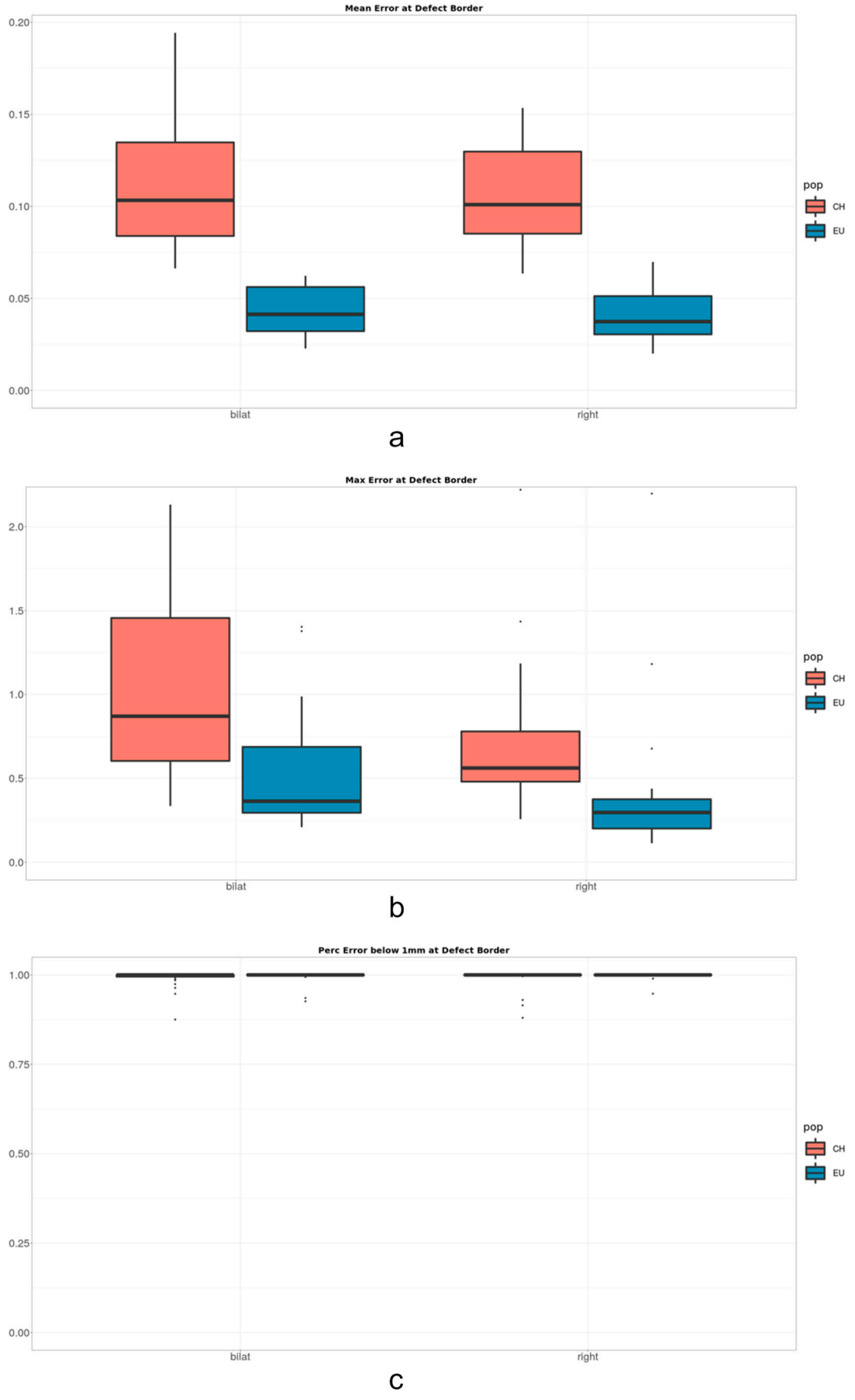

Fig. 6. Boxplots visualizing the reconstruction error distribution at the defect borders for both groups divided up in uni- and bilateral defects in mm.
Mean error distribution of the error distribution; (b) Maximum error distribution of the error distribution (c) Percentage of vertices below 1 mm at the defect borders.

populations with an average error of 0.12 mm (SD = 0.07) among Chinese and 0.04 mm (SD = 0.03) in Europeans. The *t*-test confirmed this, reporting a *p*-value of $3.2*10^{-10}$. The maximum errors at the border are also higher in Chinese as well with 0.8 mm (SD = 0.74) vs. 0.42 mm (SD = 0.53) in Europeans ($p = 0.047$). Regarding the number of vertices below 1 mm no significant difference was found within this region.

3.2. Bilateral defect

The estimation errors of the bilateral defects are slightly higher but with a similar outcome regarding the population differences: The mean/max error throughout the entire defect is 0.52 mm/2.55 mm (SD = 0.14/0.67) for the Chinese and 0.47 mm/2.65 mm (SD = 013/0.59) among Europeans. None of the differences reach statistical significance.

This also holds true for the percentage of vertices with an error below 1 mm that is 85 % in Chinese and 87 % in Europeans.

Again, the errors at the defect border are higher in Chinese with mean/max values of 0.13 mm/1.17 mm (SD = 0.08/0.92) while the estimation errors are significantly lower for Europeans with 0.5 mm/0.47 mm (SD = 0.04/0.63). *t*-Tests report *p*-values of $4.3 * 10^{-10}$ for the mean errors and 0.01 for the maximum errors.

4. Discussion

In this study we could show that for reconstructing large defects in the cranial vault using a SSMtrained on European data works almost as weonard.brandenburg@uniklinik-freiburg.dell on a Chinese population as it does on data from the original population. Unfortunately, we did not have access to a sufficient amount Chinese data to train a model that was comparable to the one used in this publication, so our result can only show one way. While there have been multiple approaches to use SSMs in virtual surgery planning (Fuessinger et al., 2018; Iannotti et al., 2014; Poltaretskyi et al., 2017), this paper is – to our knowledge – the first that attempts to assess the application of a population specific model to another morphologically distinct population (Rüdell and Schlager, 2013; Schlager and Rüdell, 2015). We are well aware that these results are only valid for the tested populations but given the morphological differences between those populations we hypothesize that our approach would also work for other human populations. Especially the accuracy of the reconstruction of the boundary of the defect - with a mean error of 0.13 mm - is precise enough for a clinical application, so that the manufacturing of patient specific implants (PSI) can be done precisely. The slightly increased deviations of the test group compared to the control group are within 0.13 mm and clearly below the blur resulting from imaging alone (Lüthi et al., 2009; Schlager and Statismo, 2015; Semper-Hogg et al., 2017).

The cause for this universal applicability of our approach is most likely owed to two factors and we doubt that it would hold true in other regions as well:

First, the neurocranium is a relatively smooth and simple convex shape (when compared to other structures like midfacial morphology) and the overall modes of variation seem already captured sufficiently by our European training sample.

Second, the last step, that tries to fit the SSM instance to the target skull, is designed as a robust deformation considering the actual morphology of the skull to be reconstructed. If the SSM instance is sufficiently close to the target shape, this last action seems to be adequate to guarantee a close fit.

5. Conclusion

SSM based reconstruction approaches are not necessarily limited to the population where the training data derives from. The prediction accuracy of the outer surface of the neurocranium is sufficient for clinical application such as automatic reconstruction procedures for patient specific implants, regardless of the patient's ancestry.

CRediT authorship contribution statement

Marc Anton Fuessinger: Writing – original draft, Methodology, Conceptualization, Data curation. **Marc Christian Metzger:** Conceptualization, Resources, Writing – review & editing, Supervision. **Rene Rothweiler:** Writing – review & editing, Resources. **Leonard Brandenburg:** Writing – review & editing, Resources. **Stefan Schlager:** Formal analysis, Methodology, Software, Validation.

Declaration of competing interest

The authors declare that they have no conflict of interest.

Acknowledgements

Funding

There was no funding of this study.

Availability of data and material

All data can be checked.

Code availability

Can be requested.

Ethics approval

Institutional ethics committee approval (450/15) by the University of Freiburg, Germany. All applicable international, national, and/or institutional guidelines for the care and use of animals were followed.

Consent for participate

Anonymized data.

Consent for publication

All authors have viewed and agreed to the submission.

References

Agbolade, O., Nazri, A., Yaakob, R., Ghani, A.A., Cheah, Y.K., 2020. Morphometric approach to 3D soft-tissue craniofacial analysis and classification of ethnicity, sex, and age. PloS One 15, e0228402.

Bravo-Hammett, S., Nucci, L., Christou, T., Aristizabal, J.F., Kau, C.H., 2020. 3D analysis of facial morphology of a colombian population compared to adult caucasians. Eur. J. Dent. 14, 342–351.

Bredbenner, T.L., et al., 2010. Statistical shape modeling describes variation in tibia and femur surface geometry between control and incidence groups from the osteoarthritis initiative database. J. Biomech. 43, 1780–1786.

Bruns, N., 2020. Blender. Unfallchirurg 123, 747–750.

Chim, H., Schantz, J.T., 2005. New frontiers in calvarial reconstruction: integrating computer-assisted design and tissue engineering in cranioplasty. Plast. Reconstr. Surg. 116, 1726–1741.

Dao Trong, P., Jesser, J., Schneider, T., Unterberg, A., Beynon, C., 2020. Interracial anatomical differences in the transsphenoidal approach to the sellar region. Br. J. Neurosurg. 1–4.

de Azevedo, S., Quinto-Sánchez, M., Paschetta, C., González-José, R., 2017. The first human settlement of the New World: a closer look at craniofacial variation and evolution of early and late holocene native american groups. Quat. Int. 431, 152–167.

Elliott, M., Collard, M., 2009. FORDISC and the determination of ancestry from cranial measurements. Biol. Lett. 5, 849–852.

Eufinger, H., Wehmoller, M., 1998. Individual prefabricated titanium implants in reconstructive craniofacial surgery: clinical and technical aspects of the first 22 cases. Plast. Reconstr. Surg. 102, 300–308.

Fedorov, A., et al., 2012. 3D slicer as an image computing platform for the quantitative imaging network. Magn. Reson. Imaging 30, 1323–1341.

Fuessinger, M.A., et al., 2018. Planning of skull reconstruction based on a statistical shape model combined with geometric morphometrics. Int. J. Comput. Assist. Radiol. Surg. 13, 519–529.
Fuessinger, M.A., et al., 2019. Virtual reconstruction of bilateral midfacial defects by using statistical shape modeling. J. Cranio-Maxillofac. Surg. 47, 1054–1059.
Galland, M., Friess, M., 2016. A three-dimensional geometric morphometrics view of the cranial shape variation and population history in the New World. Am. J. Hum. Biol. Off. J. Hum. Biol. Counc. 28, 646–661.
Galloway, F., et al., 2013. A large scale finite element study of a cementless osseointegrated tibial tray. J. Biomech. 46, 1900–1906.
Goodall, C., 1991. Procrustes methods in the statistical analysis of shape. J. R. Stat. Soc. Ser. B Methodol. 53, 285–321.
Harvati, K., Weaver, T.D., 2006. Human cranial anatomy and the differential preservation of population history and climate signatures. Anat Rec A Discov Mol Cell Evol Biol 288, 1225–1233.
Hubbe, M., Strauss, A., Hubbe, A., Neves, W.A., 2015. Early south americans cranial morphological variation and the origin of american biological diversity. PloS One 10, e0138090.
Iannotti, J., et al., 2014. Three-dimensional preoperative planning software and a novel information transfer technology improve glenoid component positioning. J. Bone Joint Surg. Am. 96, e71.
Kikinis, R., Pieper, S.D., Vosburgh, K.G., 2014. 3D slicer: A platform for subject-specific image analysis, visualization, and clinical support. In: Jolesz, F.A. (Ed.), Intraoperative Imaging and Image-Guided Therapy. Springer New York, pp. 277–289.
Kim, S.-G., et al., 2012. Development of 3D statistical mandible models for cephalometric measurements. Imaging Sci. Dent. 42, 175–182.
Lüthi, M., Albrecht, T., Vetter, T., 2009. In: Building Shape Models From Lousy Data. Springer, pp. 1–8.
Lüthi, M., Blanc, R., Albrecht, T., 2012. Statismo - a framework for PCA based statistical models. Insight J. (ISSN 2327-770X).
Marreiros, F.M., Heuzé, Y., Verius, M., Unterhofer, C., Freysinger, W., Recheis, W., 2016 Dec. Custom implant design for large cranial defects. Int. J. Comput. Assist. Radiol. Surg. 11 (12), 2217–2230. https://doi.org/10.1007/s11548-016-1454-8. Epub 2016 Jun 29. PMID: 27358081.
Mashiko, T., Minabe, T., Ohnishi, F., Momosawa, A., 2019. Restoration of bilateral cranial defects by hybridization of microvascular free flaps and artificial bones. Plast. Reconstr. Surg. Glob. Open 7, e2428.
Mitchell, K.S., et al., 2020. First-in-human experience with integration of wireless intracranial pressure monitoring device within a customized cranial implant. Oper. Neurosurg. Hagerstown. https://doi.org/10.1093/ons/opz431.
Mutsvangwa, T., Burdin, V., Schwartz, C., Roux, C., 2015. An automated statistical shape model developmental pipeline: application to the human scapula and humerus. IEEE Trans. Biomed. Eng. 62, 1098–1107.
Piazza, M., Grady, M.S., 2017. Cranioplasty. Neurosurg. Clin. N. Am. 28, 257–265.
Poltaretskyi, S., et al., 2017. Prediction of the pre-morbid 3D anatomy of the proximal humerus based on statistical shape modelling. Bone Jt. J 99, 927–933.
R Development Core Team, 2011. R: A Language and Environment for Statistical Computing.
Rüdell, A., Schlager, S., 2013. Shape analysis of the human zygomatic bone - data evaluation. Am. J. Phys. Anthropol. 150, 238.
Schlager, S., Rüdell, A., 2015. Analysis of the human osseous nasal shape - population differences and sexual dimorphism. Am. J. Phys. Anthropol. 157, 571–581.
Schlager, S., Statismo, T., 2015. RvtkStatismo: Integrating statismo and R using the vtkStandardMeshRepresenter.
Semper-Hogg, W., et al., 2017. Virtual reconstruction of midface defects using statistical shape models. J. Cranio-Maxillofac. Surg. 45, 461–466.
Zhang, D., Wang, S., Li, J., Zhou, Y., 2018. Novel method of constructing a stable reference frame for 3-dimensional cephalometric analysis. Am. J. Orthod. Dentofac. Orthop. 154, 397–404.